Automated Synthesis of [18F](*2S,4R*)-4-fluoroglutamine on a GE FX-N Pro Module

Xiang Zhang[1], **Falguni Basuli**[1], **Zhen-Dan Shi**[1], **Biying Xu**[1], **Burchelle Blackman**[1], **Peter L. Choyke**[2], and **Rolf E. Swenson**[1,*]

[1]Imaging Probe Development Center, National Heart, Lung, and Blood Institute, National Institutes of Health, Rockville, MD, USA

[2]Molecular Imaging Program, National Cancer Institute, National Institutes of Health, Bethesda, MD, USA

Abstract

Glutamine (Gln) and its analogues may serve as imaging agents for tumor diagnosis using positron emission tomography (PET), especially for tumors with negative [18F]FDG scan. We report the first automated synthesis of [18F](*2S,4R*)-4-fluoroglutamine ([18F]FGln) on a GE FX-N Pro synthesizer. [18F]FGln was obtained in 80 min with a radiochemical yield of $21 \pm 3\%$ (n = 5, uncorrected). The radiochemical purity was $> 98\%$, and optical purity $90 \pm 5\%$. The synthesis is highly reproducible with good chemical purity, radiochemical yield, and is suitable for translation to cGMP production.

Keywords

fluoroglutamine; F-18; automation; PET imaging; tumor

1. Introduction

Glutaminolysis is an alternative source of metabolic energy for tumor cells (Gaglio et al., 2011; Lieberman et al., 2011; Liu et al., 2012; Wang et al., 2010). Therefore, glutamine (Gln) and its analogues may serve as potential imaging agents for tumor diagnosis using positron emission tomography (PET), especially for tumors with negative [18F]FDG scan. Recently, Hank et al. reported an F-18 labeled Gln analogue [18F](*2S,4R*)-4-fluoroglutamine ([18F]FGln, [18F]**1**) (Qu et al., 2011). It showed specific uptake in both *in vitro* tumor cells and PET imaging of tumor bearing animal models (Hassanein et al., 2015; Lieberman et al., 2011; Ploessl et al., 2012). The clinical evaluation of [18F]**1** in human glioma patients also demonstrated good uptake and a high tumor:background ratio (Venneti et al., 2015). Although *in vivo* defluorination was detected (Wu et al., 2014), multiple studies in rodent

and human species have demonstrated the level of free fluoride is low enough not to interfere with [^{18}F]**1** uptake in various organs, or hamper imaging (Hassanein et al., 2015; Venneti et al., 2015). These studies and others have established that PET imaging with [^{18}F]**1** is a highly attractive approach for clinical tumor diagnosis and therapy evaluation.

The manual synthesis of [^{18}F]**1** has been reported previously (Lieberman et al., 2011; Qu et al., 2011; Venneti et al., 2015). The reported radiochemical yield is 8–10% (uncorrected) with > 98% radiochemical purity (RCY) and > 82% optical purity. Since the clinical potential of this PET tracer is being recognized, the demand for [^{18}F]**1** may increase. Therefore there are clear benefits to further optimizing and automating the synthesis for more efficient and routine production. Here, we report a method to optimize the synthesis of [^{18}F]**1**, and adapt it to automated production on a GE FX-N Pro module.

2. Materials and Methods

2.1. General

Unless otherwise noted, all chemicals and solvents were purchased from Sigma-Aldrich (Milwaukee, WI, USA) or Fisher Scientific (Hanover Park, IL, USA) and used without further purification. (*S*)-4-*tert*-butyl- 2-(*tert*-butoxycarbonylamino)-4-hydroxybutanoate was purchased from Aldlab Chemicals, LLC (Woburn, MA, USA). Non-carrier added [^{18}F]fluoride was obtained from the National Institutes of Health cyclotron facility (Bethesda, MD, USA). Chromafix® PS-HCO$_3$ cartridges (45 mg) were purchased from Macherey-Nagel Inc (Dueren, Germany). Oasis HLB light cartridges were obtained from Waters (Milford, MA, USA). Sterile Millex-GS filter (catalog: SLGSV255F, 0.22 μm × 25 mm) was purchase from EMD Millipore (Billerica, MA, USA). USP grade absolute ethanol was purchased from VWR International (Radnor, PA, USA). Sterile 10 mL vial was purchased from Hospira (Lake Forest, IL, USA). Water was purified by a MilliQ integral water purification system. PTFE coated septa for the GL-14 Cap (catalog: CG-196-10) was obtained from Chemglass (Vineland, NJ, USA). D$_2$O was purchased from Cambridge Isotope Laboratories, Inc (Andover, MA, USA).

Semi-preparative high-pressure liquid chromatography (HPLC) was conducted in the GE TRACERlab™ FX-N Pro under the following HPLC condition: Agilent XDB-C18 column, 250 × 10 mm, 5 μM; mobile phase: 73.5% MeOH and 26.5% Water (+0.1% v/v formic acid); 4 mL/min. Analytical HPLC was performed using an Agilent 1260 HPLC system, which includes a quaternary gradient pump, a variable wavelength detector, and a Bioscan radioactivity-HPLC-flow detector. Analytical HPLC was performed to check the identity of the intermediate ([^{18}F]**3**) and residual anisole under the following condition: Agilent Eclipse XDB C18 4.6 × 150 mm, 5 μm, 75% MeOH and 25% Water (+0.1% v/v formic acid), 1 mL/min. The enantiomeric purity of the final [^{18}F]**1** was confirmed under the following chiral HPLC condition: Chirex 3126 (d)-penicillamine, 1 mM CuSO$_4$, 1 mL/min. ^{19}F-NMR was recorded on a Bruker 400 MHz NMR spectrometer (Billerica, MA, USA).

2.2. Elution of fluorine-18

The elution efficiency of fluorine-18 from a Chromafix® PS-HCO$_3$ cartridge was evaluated with KHCO$_3$ and Kryptofix 2.2.2 or 18-crown-6. ACN/H$_2$O or MeOH/H$_2$O was used as the eluent for eluting trapped fluorine-18 from a PS-HCO$_3$ cartridge.

2.3. Module preparation and hardware modification

The optimized radiosynthesis of [^{18}F]**1** was completed via the following procedure: fluorination, HPLC purification, hydrolysis, and formulation. In order to perform the hydrolysis in reactor 2 (R2) after HPLC purification of the intermediate compound, we implemented slight adjustments to the tubing connection of the FX-N Pro module. V15-normally close (NC) was connected to V35, which was used to elute the purified intermediate [^{18}F]**3** from the HLB light cartridge directly to R2. In addition, V16 (Al$_2$O$_3$ #2) was connected through a 0.22 μm Millex-GS filter to a 10 mL sterile vial as the product delivery loop. The detailed diagram of the control interface is shown in Figure 1.

The synthesis of [^{18}F]**1** consists of 11 reagent vials on the FX-N Pro module. Vials 1-5 were used for the elution, drying of F-18, and fluorination reaction. Vials 13–14 were used for the formulation of purified [^{18}F]**3**, and vials 7–10 for the hydrolysis and formulation of final product [^{18}F]**1**. Specifically, Vial 1 was added with KHCO$_3$ (0.18 mL, 8 mg/mL in water) and 18-crown-6 (8 mg) solution in MeOH (1.0 mL); Vial 2 was added with ACN (1 mL); Vial 3 was added with the tosylate precursor **2** (5 mg) in ACN (0.6 mL); Vial 4 was added with water (0.6 mL); Vial 5 was added with HPLC solvent (3.0 mL); Vial 7 was added with PBS pH 7.4 (2.0 mL); Vial 8 was added with PBS pH 7.4 (1.0 mL); Vial 9 was added with EtOH (1.0 mL); Vial 10 was added with trifluoroacetic acid (TFA, 1.0 mL)/anisole (10 μL); Vial 13 was added with EtOH (1.0 mL); Vial 14 was added with water (6 mL); HPLC dilution flask was added with water (18 mL). Note that Vial 10 was used for TFA/anisole solution, the original blue septum was changed to PTFE coated septum for better chemical resistance.

2.4. Radiosynthesis of [^{18}F]1

Typically, 3.7 GBq (100 mCi) [^{18}F]fluoride in 2.5 mL of water was passed through the PS-HCO$_3$ cartridge, and the cartridge was rinsed with 1 mL of acetonitrile. [^{18}F]fluoride was eluted from the cartridge into reactor 1 (R1) with the eluent in Vial 1, and dried under N$_2$/vacuum at 75 °C for 4 min. R1 was cooled to 50 °C, acetonitrile in Vial 2 was added and the activity was azeotropically dried at 55 °C for 3 min and at 95 °C for 3 min under N$_2$/vacuum. The activity was further dried using a vacuum for 3 min. The [^{18}F]fluoride drying cycle took about 20 min.

The tosylate precursor **2** in Vial 3 was added to the dried activity. The resulting solution was stirred at 70 °C for 15 min, cooled to 45 °C. The reaction mixture was diluted with 0.6 mL of water (Vial 4), and transferred in Tube 2. R1 was rinsed with HPLC mobile phase (Vial 5) and the solution was also transferred to Tube 2. The solution in Tube 2 was thoroughly mixed by bubbling N$_2$ for 10 seconds and injected into the HPLC for purification. The labeled product was eluted at about 12–13 min, the precursor was eluted at 19–20 min (Figure S1). The product peak was collected in the dilution flask containing 18 mL water,

and passed through an Oasis HLB light cartridge (pre-conditioned with 5 mL of ethanol, 10 mL of air, and 10 mL of water). The trapped intermediate was rinsed with 6 mL water (Vial 14), and eluted with 1.0 mL of absolute ethanol (Vial 13) to R2 through V35.

The eluted intermediate was heated to 60 °C under N_2 flow and vacuum for 3 min to remove ethanol. TFA/anisole mixture (1 ml/10 μL, Vial 10) was added to the dried residue. The resulting solution was heated at 60 °C for 5 min. The volatiles were removed under vacuum and N_2 for 3 min, followed by vacuum only for 1 min. Ethanol (1 mL, Vial 9) was added, the volatile was again evaporated under vacuum/N_2 for 3 min, vacuum only for 1 min to completely remove the acidic volatiles. The dried activity was cooled down to 45 °C, and 1.0 mL PBS buffer (pH 7.4, Vial 8) was added. The content was transferred through V16 and an in-line sterile filter to the product vial. R2 was rinsed with 2.0 mL PBS buffer (pH 7.4, Vial 7) and the solution was transferred to the product vial.

2.5. Product characterization and stability study

The chemical identity of the fluorinated intermediate ($[^{18}F]$**3**) was checked by analytical HPLC, the retention time of $[^{18}F]$**3** is 6.5–6.7 min. The enantiomeric purity of the final $[^{18}F]$**1** was confirmed by chiral HPLC, which was eluted at 9.0–9.5 min. The residual anisole in the final dose was analyzed by analytical HPLC, the concentration was obtained by fitting to a calibration curve of standard anisole solution (0.5, 1.0, 2.5, 5.0, 10 ppm). ^{19}F-NMR experiment was performed to check the TFA residue in the fully-decayed product sample. The NMR samples of the product solution and TFA standards (1, 10, 100, 1,000 ppm) were prepared by adding 100 μL of D_2O to 600 μL of the solution, which was mixed on a vortex for 10 s. ^{19}F-NMR spectra were obtained and the TFA peak was integrated. A calibration curve of peak area vs. standard concentration was constructed. The TFA concentration of the product sample was quantified by fitting the peak area to the calibration curve.

For in vial stability, a sample of $[^{18}F]$**1** (3.7 MBq in 100 μL PBS pH 7.4 buffer) was kept under room temperature for 4 h and analyzed by chiral HPLC. For *in vitro* stability, 3 samples of $[^{18}F]$**1** (0.37 MBq in 10 μL PBS pH 7.4 buffer) were added to mouse serum (100 μL), incubated at 37 °C for 30 min, 1 h and 2 h. At each time point, 110 μL of ACN was added to the sample. The mixture was spun at 12,000 g for 5 min, and the supernatant was collected. A 1 mM $CuSO_4$ solution (80 μL) was added to the collected supernatant (20 μL). The solution (100 μL) was injected for HPLC analysis.

3. Results and Discussion

3.1. Chemical synthesis

The optically pure precursor, *tert*-butyl-(2*S*,4*S*)-2-((*tert*-butoxycarbonyl)amino)-5-oxo-4-(tosyloxy)-5-((2,4,6-trimethoxybenzyl)amino)pentanoate (**2**) and nonradiolabeled reference standard **1** were synthesized following the literature method with slight changes (Qu et al., 2011). According to the literature, the intermediate (*S*)-4-*tert*-butyl-2-(*tert*-butoxycarbonylamino)-4-oxobutanoate was synthesized in five steps. In our synthesis, it was

prepared in one step by Dess-Martin oxidation of commercially available (*S*)-4-*tert*-butyl-2-(*tert*-butoxycarbonylamino)-4-hydroxybutanoate.

3.2. Optimization of the radiosynthesis

The radiosynthesis of [^{18}F]**1** is shown in Scheme 1. The selection and concentration of the base is an important factor for efficient F-18 labeling, as the reaction is sensitive to strong basic condition. It was reported that under basic conditions of K_2CO_3 and K_{222}, epimerization occurs, which may potentially lead to all 4 stereo-isomers of **1** (Qu et al., 2011). However, if only a limited amount of base or a weak base is added it may not efficiently elute F-18 from the anion exchange cartridge in an automated process. Therefore, a proper balance between the selection of base and F-18 elution efficiency is critical in order to maximize the yield during automation. In this regard, we further optimized the base/phase transfer catalyst system based on the reported condition (Table 1). As the initial screening, K_{222} was tested with weak base $KHCO_3$ (1.5 mg) in a mixture of acetonitrile and water, which gave 80–82% of F-18 recovery from PS-HCO$_3$ cartridge, but chiral HPLC of the final [^{18}F]**1** sample demonstrated the formation of all 4 stereo-isomers, resulting in only 40–47% optical purity (Table 1 entry 1). When K_{222} was replaced with 18-crown-6, the unwanted epimerization was substantially decreased. Reproducible results were obtained with >85% optical purity which was in agreement with the literature. However, F-18 elution was not ideal with only up to 85% recovery after elution (Table 1 entries 2–3). Based on a recent publication by Moon et al., we tested methanol instead of ACN as the eluent (Moon et al., 2010); superior elution efficiency was obtained with 1.44 mg of $KHCO_3$ in MeOH (> 95% eluted, Table 1 entry 4). This process displayed high reproducibility in both elution efficiency and optical purity of the final product.

In previously reported syntheses, a solid phase extraction (SPE) method was used to purify the intermediate [^{18}F]**3**. However, this process cannot fully remove the UV impurities and unreacted precursor **1** from the labeled intermediate, resulting in low chemical purity of the product. In addition, upon quenching the fluorination reaction with water, it occasionally forms a precipitate which may block the cartridge and lower the reproducibility on an automated module. In our attempt to optimize the reaction, we found HPLC purification of the intermediate was able to avoid the formation of precipitate. The intermediate peak was also collected with high purity, which greatly improved the feasibility of the process on the module. More importantly, the overall yield of [^{18}F]**1** was greatly improved to about 20%.

3.3. Automated synthesis and formulation

Using the optimized condition, the 2-step automated synthesis of [^{18}F]**1** was performed on a GE FX-N Pro module (Figure 1). The GE FX-N Pro module contains two reactors to enable two-step nucleophilic fluorination. In order to support hydrolysis of the intermediate [^{18}F]**3,** after HPLC purification, slight adjustments was performed to the tubing connection. The modification provided purified [^{18}F]**3** eluted directly to R2 from the Sep-pak. In the automated synthesis, the azeotropic drying and fluorination reaction were performed in R1, and the crude [^{18}F]**3** was purified by reverse phase HPLC. The collected [^{18}F]**3** was diluted in water, trapped on a HLB light Sep-pak, eluted with EtOH in R2 for hydrolysis. The

hydrolyzed [^{18}F]**1** was reformulated in PBS (pH 7.4) and sterile filtered into the final product vial.

3.4. Characterization of [^{18}F]1 and Stability test

Starting from 3.7 ± 0.56 GBq (100 ± 15 mCi) of [^{18}F]F$^-$, 0.77 ± 0.15 GBq (20 ± 4 mCi) of [^{18}F]**1** was readily formulated. These amounts would be sufficient to perform PET experiments in multiple human subjects. The total synthesis time is 80 ± 3 min, the uncorrected RCY is 21 ± 3% (n = 5). Radiochemical purity was > 98% with a stereochemical purity 90 ± 5%. Anisole residue was assayed by HPLC with a standard curve. It has confirmed the level of anisole is negligible in the final dose (lower than the minimum detectable concentration 0.5 ppm). The residue of TFA was quantified by ^{19}F-NMR experiment of the fully-decayed product, which found a TFA residue of 50.7 ppm in the final dose. However, TFA is listed under "other residue solvents" according to US Pharmacopeia, no adequate toxicological data is available to determine the Permitted Daily Exposure (2015).

The stability of [^{18}F]**1** was tested in vial and in mouse serum. In PBS pH 7.4 buffer, [^{18}F]**1** is stable for up to 4 h at room temperature, no decomposition was detected. *In vitro* stability study of [^{18}F]**1** was checked by incubating the labeled product with mouse serum under 37 °C. The experiment showed that[^{18}F]**1** remains >98% intact in mouse serum after 2 h, and no defluorination was detected.

4. Conclusion

We have optimized the radiosynthesis of [^{18}F]**1**, and translated the radiosynthesis to a fully-automated commercial synthesis box. This procedure allows for the efficient and reproducible synthesis of this tracer. [^{18}F]**1** was obtained in high radiochemical yield and radiochemical purity for PET experiments. Key features of our automated synthesis include the use of KHCO$_3$ in methanol, instead of acetonitrile to elute the final product. We also found that purification of the intermediate compound by reverse phase HPLC was superior to the SPE method reported previously. The production could be easily adapted to cGMP productions for routine clinical use, enabling wide-spread access to this promising PET tracer.

Supplementary Material

Refer to Web version on PubMed Central for supplementary material.

Acknowledgments

References

United States Pharmacopeia. National Formulary. 2015; 38

Gaglio D, Metallo CM, Gameiro PA, Hiller K, Danna LS, Balestrieri C, Alberghina L, Stephanopoulos G, Chiaradonna F. Oncogenic K-Ras decouples glucose and glutamine metabolism to support cancer cell growth. Mol Syst Biol. 2011; 7:523. [PubMed: 21847114]

Hassanein M, Hight MR, Buck JR, Tantawy MN, Nickels ML, Hoeksema MD, Harris BK, Boyd K, Massion PP, Manning HC. Preclinical Evaluation of 4-[F]Fluoroglutamine PET to Assess ASCT2 Expression in Lung Cancer. Molecular imaging and biology : MIB : the official publication of the Academy of Molecular Imaging. 2015

Lieberman BP, Ploessl K, Wang L, Qu W, Zha Z, Wise DR, Chodosh LA, Belka G, Thompson CB, Kung HF. PET imaging of glutaminolysis in tumors by 18F-(2S,4R)4- fluoroglutamine. J Nucl Med. 2011; 52:1947–1955. [PubMed: 22095958]

Liu W, Le A, Hancock C, Lane AN, Dang CV, Fan TW, Phang JM. Reprogramming of proline and glutamine metabolism contributes to the proliferative and metabolic responses regulated by oncogenic transcription factor c-MYC. Proc Natl Acad Sci U S A. 2012; 109:8983–8988. [PubMed: 22615405]

Moon BS, Park JH, Lee HJ, Kim JS, Kil HS, Lee BS, Chi DY, Lee BC, Kim YK, Kim SE. Highly efficient production of [(18)F]fallypride using small amounts of base concentration. Appl Radiat Isot. 2010; 68:2279–2284. [PubMed: 20609592]

Ploessl K, Wang L, Lieberman BP, Qu W, Kung HF. Comparative evaluation of 18F-labeled glutamic acid and glutamine as tumor metabolic imaging agents. J Nucl Med. 2012; 53:1616–1624. [PubMed: 22935578]

Qu WC, Zha ZH, Ploessl K, Lieberman BP, Zhu L, Wise DR, Thompson CB, Kung HF. Synthesis of Optically Pure 4-Fluoro-Glutamines as Potential Metabolic Imaging Agents for Tumors. J Am Chem Soc. 2011; 133:1122–1133. [PubMed: 21190335]

Venneti S, Dunphy MP, Zhang H, Pitter KL, Zanzonico P, Campos C, Carlin SD, La Rocca G, Lyashchenko S, Ploessl K, Rohle D, Omuro AM, Cross JR, Brennan CW, Weber WA, Holland EC, Mellinghoff IK, Kung HF, Lewis JS, Thompson CB. Glutamine-based PET imaging facilitates enhanced metabolic evaluation of gliomas in vivo. Sci Transl Med. 2015; 7:274ra217.

Wang JB, Erickson JW, Fuji R, Ramachandran S, Gao P, Dinavahi R, Wilson KF, Ambrosio AL, Dias SM, Dang CV, Cerione RA. Targeting mitochondrial glutaminase activity inhibits oncogenic transformation. Cancer Cell. 2010; 18:207–219. [PubMed: 20832749]

Wu Z, Zha Z, Li G, Lieberman BP, Choi SR, Ploessl K, Kung HF. [(18)F](2S,4S)-4-(3-Fluoropropyl)glutamine as a tumor imaging agent. Mol Pharm. 2014; 11:3852–3866. [PubMed: 25095908]

Highlights

- The radiosynthesis of [^{18}F]fluoroglutamine was optimized with improved yield and purity.

- Fully automated synthesis was established on a GE FX-N Pro module.

- Radiochemical yield of 21 ± 3% (uncorrected, n = 5) was obtained with good reproducibility.

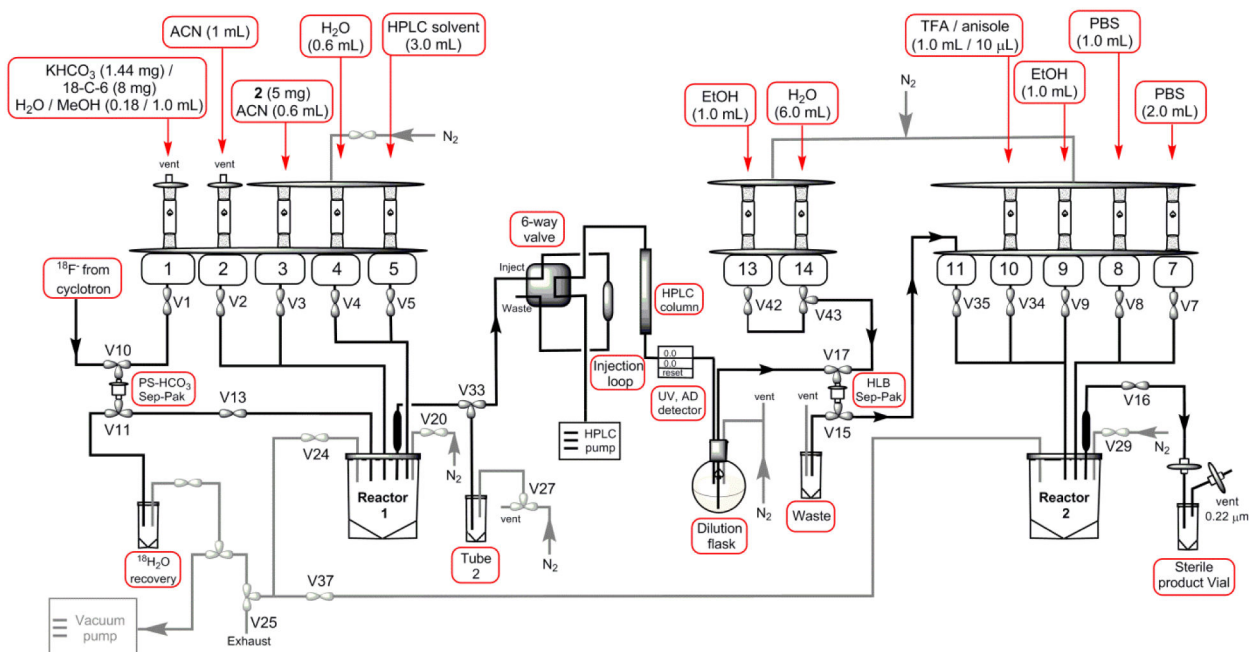- The automation could be easily adapted to cGMP production for routine clinical use.

Figure 1.
Schematic diagram of the GE TRACERlab FX-N Pro Module. The flow paths were shown by arrows and important valves were labeled. The following connections were modified to be suitable for the synthesis: V15-NC was connected to V35 for transferring the purified intermediate [^{18}F]**3** to R2; V16 was connected to the product delivery line for transferring the final product.
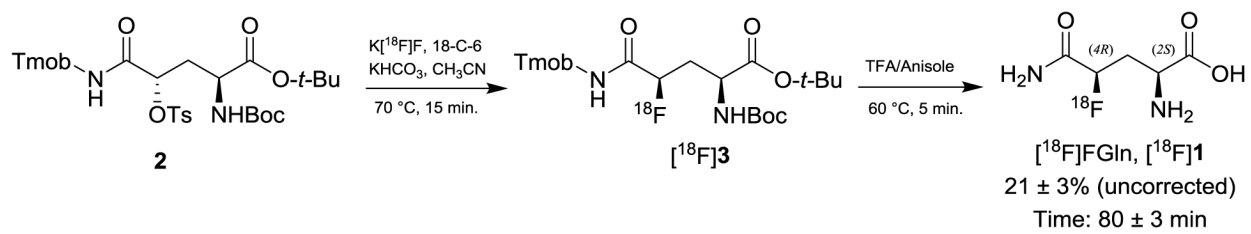
Scheme 1.
Radiosynthesis of [^{18}F]**1**.

Table 1

Optimization of base, phase-transfer agent and eluting solvent

entry	base/phase-transfer agent (mg/mg)	Solvent (v/v)	^{18}F elution efficiency (%)	enantiomeric purity of the product (%)[c]
1	KHCO$_3$/K$_{222}$ (1.5/5)[a]	ACN/H$_2$O (1/0.3)	80–82	40–47 (n = 2)
2	KHCO$_3$/18-C-6 (1.5/8)[a]	ACN/H$_2$O (1/0.3)	82	92
3	KHCO$_3$/18-C-6 (2.0/8)[b]	ACN/H$_2$O (1/0.25)	85	87
4	KHCO$_3$/18-C-6 (1.44/8)[b]	MeOH/H$_2$O (1/0.18)	> 95	85–93 (n = 5)

[a] 5 mg/mL KHCO$_3$ solution was used.

[b] 8 mg/mL KHCO$_3$ solution was used.

[c] Enantiomeric purity was obtained on analytical chiral HPLC of the final product: Chiral Chirex 3126 (D-penicillamine) (150 × 4.6 mm); Mobile phase: 1 mM CuSO$_4$, 1 mL/min.